Atp6ap2 deletion causes extensive vacuolation that consumes the insulin content of pancreatic β cells

Katrina J. Binger[a,b,1,2], Martin Neukam[c,2], Sudhir Gopal Tattikota[d,e], Fatimunnisa Qadri[e,f], Dmytro Puchkov[g], Diana M. Willmes[c], Sabrina Wurmsee[e,f], Sabrina Geisberger[e,f], Ralf Dechend[f], Klemens Raile[f], Thomas Kurth[h], Genevieve Nguyen[i], Matthew N. Poy[e,j], Michele Solimena[c,2], Dominik N. Muller[e,f,2], and Andreas L. Birkenfeld[c,k,l,m,2]

[a]Department of Biochemistry and Genetics, La Trobe Institute for Molecular Sciences, La Trobe University, Bundoora, VIC 3086, Australia; [b]Department of Biochemistry and Molecular Biology, Bio21 Molecular Science and Biotechnology Institute, The University of Melbourne, Parkville, VIC 3010, Australia; [c]Molecular Diabetology, Paul Langerhans Institute Dresden (PLID) of the Helmholtz German Center for Diabetes Research (DZD e.V.) Munich, University Hospital Carl Gustav Carus and Faculty of Medicine, TU Dresden, 01307 Dresden, Germany; [d]Department of Genetics, Harvard Medical School, Boston, MA 02115; [e]Cardiovascular and Metabolic Diseases, Max Delbruck Center (MDC) for Molecular Medicine in the Helmholtz Association, 13125 Berlin, Germany; [f]Experimental and Clinical Research Center, Charité–Universitätsmedizin Berlin and Max Delbruck Center for Molecular Medicine, 13125 Berlin, Germany; [g]Cellular Imaging Facility, Leibniz Institute for Molecular Pharmacology (FMP) Berlin, 13125 Berlin, Germany; [h]Center for Molecular and Cellular Bioengineering, Center for Regenerative Therapies Dresden, TU Dresden, 01307 Dresden, Germany; [i]Center for Interdisciplinary Research in Biology, UMR INSERM U1050/CNRS 7241, Collège de France, 75231 Paris, France; [j]Institute for Fundamental Biomedical Research, All Children's Hospital, Johns Hopkins University, St. Petersburg, FL 33701; [k]Department of Diabetology Endocrinology and Nephrology, University Hospital Tübingen, Eberhard Karls University Tübingen, 72074 Tübingen, Germany; [l]Department of Therapy of Diabetes, Institute of Diabetes Research and Metabolic Diseases in the Helmholtz Center Munich, Eberhard Karls University Tübingen, 72074 Tübingen, Germany; and [m]Division of Diabetes and Nutritional Sciences, Rayne Institute, King's College London, London SE5 9RJ, United Kingdom

Edited by David C. Rubinsztein, University of Cambridge, Cambridge, United Kingdom, and accepted by Editorial Board Member F. Ulrich Hartl August 17, 2019 (received for review March 21, 2019)

Pancreatic β cells store insulin within secretory granules which undergo exocytosis upon elevation of blood glucose levels. Crinophagy and autophagy are instead responsible to deliver damaged or old granules to acidic lysosomes for intracellular degradation. However, excessive consumption of insulin granules can impair β cell function and cause diabetes. *Atp6ap2* is an essential accessory component of the vacuolar ATPase required for lysosomal degradative functions and autophagy. Here, we show that Cre recombinase-mediated conditional deletion of *Atp6ap2* in mouse β cells causes a dramatic accumulation of large, multigranular vacuoles in the cytoplasm, with reduction of insulin content and compromised glucose homeostasis. Loss of insulin stores and gigantic vacuoles were also observed in cultured insulinoma INS-1 cells upon CRISPR/Cas9-mediated removal of *Atp6ap2*. Remarkably, these phenotypic alterations could not be attributed to a deficiency in autophagy or acidification of lysosomes. Together, these data indicate that *Atp6ap2* is critical for regulating the stored insulin pool and that a balanced regulation of granule turnover is key to maintaining β cell function and diabetes prevention.

autophagy | (pro)renin receptor | diabetes | vacuolar H^+ ATPase

Pancreatic β cells are exclusive in their role for producing insulin, and in response to increased extracellular glucose concentrations they rapidly synthesize, package, and export insulin into the systemic circulation. Proper control of each step is critical to maintain continuous insulin secretion throughout the day and is critical to preventing the onset of diabetes—a disease which affects approximately one-third of Western populations (1). Insulin is stored within secretory granules (SGs), which are small (~250 nm), membrane-enclosed structures containing crystallized insulin (2). Maintaining the integrity of SGs and the removal of aged or defective SGs are also required for preserving β cell homeostasis (3).

Autophagy is one such mechanism involved in the intracellular turnover of SGs (4). This process entails the sequestration of cytoplasmic organelles, proteins, and other cellular constituents into double-membraned autophagosomes with a neutral luminal pH. Autophagosomes then fuse with lysosomes for degradation of their content within the acidic milieu of the autophagolysosome (5). While in general, autophagy is considered protective due to its ability to remove components which could perturb homeostasis, over- and uncontrolled degradation of cellular contents can also cause significant damage. Several pieces of evidence point to the relevance of balanced autophagy for β cell homeostasis. On one hand, absence of β cell autophagy in mice lacking autophagy related 7 (*Atg7*), a protein necessary for the formation of autophagosomes, results in endoplasmic reticulum stress, impaired insulin secretion, and hyperglycemia (6, 7). On the other hand, the occurrence of increased autophagy in human (8) and rodent (7, 9) islets is also associated with the development of diabetes. Likewise, hyperactivation of autophagy following treatment with rapamycin also impairs β cell function and viability, resulting in decreased insulin secretion and diabetes (10, 11).

As lysosomal acidification is required for the degradation of the autophagolysosomal content, understanding the biology of this process is of utmost importance. The vacuolar H^+ (V)-ATPase is a large transmembrane protein complex responsible for establishing and retaining the pH gradient along the secretory, endocytic, and lysosomal pathways in all cell types. Complete loss of V-ATPase function is hence embryonic lethal (reviewed in ref. 12). The V-ATPase complex consists of 2 functional domains: V_1, consisting of 8 subunits and responsible for ATP hydrolysis; and V_0, with 6 to 7 membrane-embedded

Significance

Cells maintain several mechanisms to ensure their survival, including the removal of old or damaged proteins and organelles. This process must be balanced: too little turnover results in the accumulation of cellular "junk," while excessive removal can deplete the cell and organism of key components. Here, we show that *Atp6ap2* in the pancreatic β cell is essential for insulin granule turnover, as its absence resulted in the accumulation of oversized cytosolic vacuoles which conceivably account for excessive granule degradation, and thereby leads to impaired insulin secretion and diabetes.

Author contributions: K.J.B., M.N., S.G.T., M.N.P., M.S., D.N.M., and A.L.B. designed research; K.J.B., M.N., S.G.T., F.Q., D.P., D.M.W., S.W., S.G., K.R., T.K., and A.L.B. performed research; G.N. contributed new reagents/analytic tools; K.J.B., M.N., S.G.T., F.Q., D.P., D.M.W., R.D., M.N.P., M.S., D.N.M., and A.L.B. analyzed data; and K.J.B., M.S., D.N.M., and A.L.B. wrote the paper.

The authors declare no conflict of interest.

This article is a PNAS Direct Submission. D.C.R. is a guest editor invited by the Editorial Board.

[1]To whom correspondence may be addressed. Email: k.binger@latrobe.edu.au.

[2]K.J.B., M.N., M.S., D.N.M., and A.L.B. contributed equally to this work.

This article contains supporting information online at www.pnas.org/lookup/suppl/doi:10.1073/pnas.1903678116/-/DCSupplemental.

First published September 16, 2019.

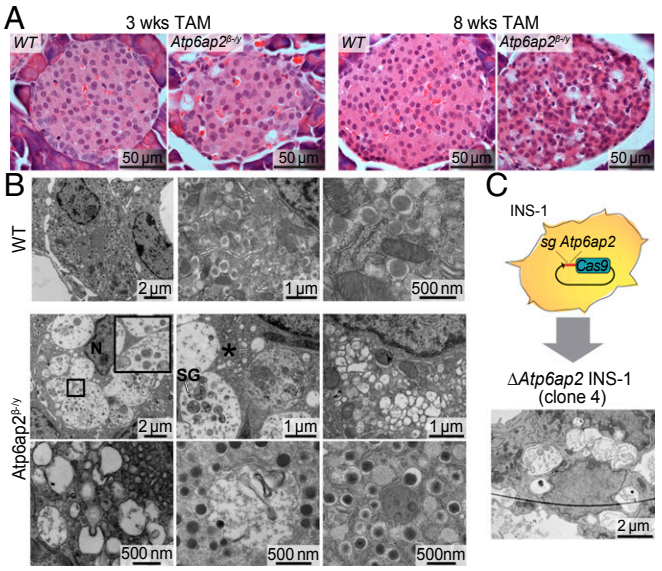

Fig. 1. *Atp6ap2* β cell deletion induces the accumulation of large vacuolated structures. (*A*) Morphological analysis by hematoxylin and eosin staining in pancreases from WT and *Atp6ap2*$^{β-/y}$ mice after TAM treatment for 3 and 8 wk. (*B*) Representative transmission electron microscopy images of β cells from WT and *Atp6ap2*$^{β-/y}$ mice after 3 wk of TAM. *Inset* shows a representative single-membraned vacuole in *Atp6ap2*$^{β-/y}$ islets. N, nucleus; SG, insulin secretory granule; *, dilated Golgi cisternae. (*C*) Rat insulinoma INS-1 cells were transfected with plasmid expressing Cas9-GFP and sgRNA targeting *Atp6ap2*. Successful clones deficient for *Atp6ap2* (Δ*Atp6ap2* INS-1 cells) were analyzed by transmission electron microscopy. Scale bars are indicated.

subunits and containing the proton-permeable pore. In yeast, V-ATPase activity is regulated by the reversible assembly and disassembly of these domains (12). In mice, loss of the V-ATPase a3 subunit causes diabetes due to impaired fusion of SGs with the plasma membrane and thus insulin release (13). Compared to yeast, higher-order eukaryotes have additional V-ATPase accessory proteins such as the ATPase H^+ Transporting Accessory Protein 1 (Atp6ap1) and 2 (Atp6ap2). Conditional depletion of Atp6ap1 (also known as Ac45) impairs the processing of proinsulin to insulin in mouse insulinoma cells (14). Atp6ap2 was initially misnamed as the (pro)renin receptor (PRR), as it was thought to bind renin and contribute to the pathology of hypertension (15, 16). Atp6ap2 has since been shown to be essential for cellular homeostasis in mice, as its knockout is embryonic lethal (17), while conditional deletion impairs the function of a variety of cell types (18–24). Its role in *Drosophila* and *Xenopus* development is also established (25–27). Atp6ap2 colocalizes with V-ATPase subunits (28, 29), and overexpression studies showed its coprecipitation with V_0 subunits (27) in association with V-ATPase dysfunction (30). Atp6ap2 has been proposed to chaperone V-ATPase assembly as its deletion causes reduced levels of V-ATPase subunits (18, 19). Other studies, however, could not show its effect on V-ATPase function (28). As deletion of *Atp6ap2* resulted in the accumulation of autophagy markers (18, 20, 24), a link with autophagy has also been suggested (31). Taken together, the precise function of Atp6ap2 remains unclear due to the severe impact that its deletion has on cellular homeostasis, with gross developmental abnormalities and cell death hindering a deeper understanding of its activity. Since Atp6ap2 is highly expressed in pancreatic β cells (32), and V-ATPase activity is necessary for the acidification of the SG lumen and insulin processing, we hypothesized that its deletion in these cells could shed light on its function.

Results

Atp6ap2$^{β-/y}$ Islets Are Consumed by Large Vacuolated Structures. To study the specific role of Atp6ap2 in pancreatic β cells, female *Atp6ap2*$^{fl/+}$ mice were mated with male mice expressing a Cre recombinase–estrogen receptor (ER) fusion protein under control of the rat insulin promoter (RIP-CreER) mice. Adult (8 wk) *RIP-CreER;Atp6ap2*$^{fl/y}$ male offspring were treated with tamoxifen (TAM) for 3 and 8 wk (*SI Appendix*, Fig. S1). Islets isolated after 3 wk TAM treatment from *RIP-CreER;Atp6ap2*$^{fl/y}$ mice (henceforth referred to as *Atp6ap2*$^{β-/y}$ mice) showed significantly decreased *Atp6ap2* mRNA and protein levels, confirming the knockout of *Atp6ap2* in β cells (*SI Appendix*, Fig. S1). The effect of *Atp6ap2* ablation was unmistakable upon histological analysis of pancreases, with heavily vacuolated cells evident within islets of *Atp6ap2*$^{β-/y}$ mice after 3 wk and, to a much greater extent, 8 wk of TAM treatment (Fig. 1*A*). To analyze these phenotypic alterations in more detail, we performed transmission electron microscopy (TEM) of islets after 3 wk of TAM treatment. WT mice showed normal morphology, with most of the β cell cytoplasm being occupied by insulin SGs (Fig. 1*B*). By contrast, the cytoplasm of *Atp6ap2*-deficient β cells was filled with large vacuolated structures, with few to no insulin SGs (Fig. 1*B*). Vacuolated structures mostly had a single outer membrane (Fig. 1 *B*, *Inset*) and contained vesicles and remnants of degraded material, including insulin SGs (*SI Appendix*, Figs. S2 and S3). In addition, several very large vesicles were observed, some of which occupied an entire β cell (*SI Appendix*, Fig. S2). Other abnormalities included dilated cisternae of the Golgi complex and large regions with small electrolucent vesicles, possibly corresponding to SGs which have lost their "dense core" (Fig. 1*B*). To exclude the possibility that such alterations resulted from off-target recombination of CreER, we used CRISPR/Cas9 technology to generate *Atp6ap2*-deficient rat insulinoma INS-1 cells. Screening for Atp6ap2 expression by Western blotting allowed the identification of 2 *Atp6ap2*-deficient INS-1 clones (#4 and #7; *SI Appendix*, Fig. S4). TEM analysis of Δ*Atp6ap2* INS-1 cells showed striking similarities to β cells of *Atp6ap2*$^{β-/y}$ mice, with their cytoplasm being almost entirely occupied by large, single-membraned vacuolated structures containing vesicles and debris, and their number of SGs being strongly reduced (Fig. 1*C*).

Atp6ap2$^{β-/y}$ Mice Have Severe Diabetes. Next, we evaluated the effect of *Atp6ap2* deletion in β cells on glucose homeostasis. Treatment of *Atp6ap2*$^{β-/y}$ mice with TAM for 8 wk did not alter

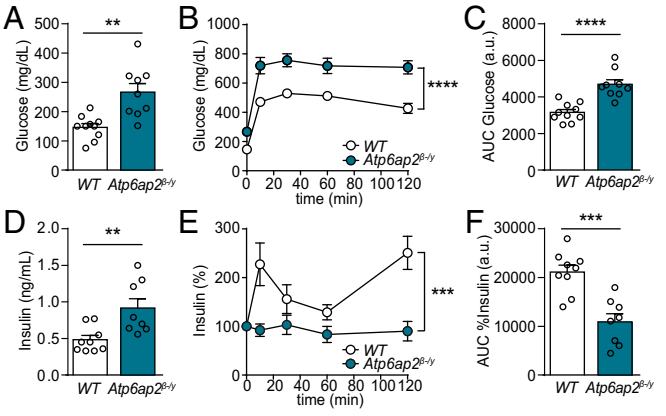

Fig. 2. Deletion of *Atp6ap2* from β cells induces severe diabetes. (*A*) Fasting blood glucose of WT and *Atp6ap2*$^{β-/y}$ mice after 8 wk of TAM treatment. (*B*) Blood glucose levels during IPGTT on adult WT and *Atp6ap2*$^{β-/y}$ mice treated with TAM for 8 wk. (*C*) Area-under-the-curve (AUC) analysis of *B*. (*D*) Fasting insulin levels of WT and *Atp6ap2*$^{β-/y}$ mice after 8 wk of TAM treatment. (*E*) Insulin levels during IPGTT as in *B*. (*F*) AUC analysis of *E*. $n = 9$ to 10. $^{**}P < 0.01$, $^{***}P < 0.001$, $^{****}P < 0.0001$.

their body weight compared to TAM-treated WT mice (*SI Appendix*, Fig. S1), while their fasting plasma glucose was significantly elevated (Fig. 2*A*). This alteration was accompanied by glucose intolerance during i.p. glucose tolerance tests (IPGTT) (Fig. 2 *B* and *C*). Specifically, in *Atp6ap2*$^{\beta\text{-}ly}$ mice, fasting plasma insulin levels were increased compared to controls (Fig. 2*D*), while glucose stimulation during IPGTT did not raise plasma insulin (Fig. 2 *E* and *F*), despite an increase of plasma glucose levels >700 mg/dL (Fig. 2*B*). These traits indicate the loss of glucose-stimulated insulin secretion (GSIS) in *Atp6ap2*$^{\beta\text{-}ly}$ mice and that knockout of *Atp6ap2* in β cells causes severe diabetes.

Decreased Insulin Content in Atp6ap2 Deficient β-Cells. *Atp6ap2*-deficient β cells could lack GSIS due to decreased insulin content and/or an impaired ability to secrete insulin. Immunofluorescence of pancreas sections after 3 wk of TAM treatment revealed a reduction in the number of insulin$^+$ cells in *Atp6ap2*$^{\beta\text{-}ly}$ mice, which was further reduced after 8 wk (Fig. 3 *A* and *B*). The decrease of insulin$^+$ cells after 8 wk of TAM treatment was coupled with an increase in the number of glucagon$^+$ cells (Fig. 3*C*). However, this increase did not originate from enhanced proliferation of α-cells, nor transdifferentiation of β cells as reporter *Atp6ap2*$^{\beta\text{-}ly}$ mice which also expressed YFP in β cells did not colocalize with glucagon (*SI Appendix*, Fig. S5). We next addressed whether there was β cell death but did not see any increase in TUNEL signal in WT or *Atp6ap2*$^{\beta\text{-}ly}$ islets (*SI Appendix*, Fig. S6). We then performed immunofluorescence for pancreatic and duodenal homeobox 1 (Pdx1), a β cell-specific transcription factor important for the maintenance of β cell identity, thus, an alternative, nucleus-specific marker for pancreatic β cells (Fig. 3*D*). No difference in Pdx1 staining was observed between pancreases of TAM-treated WT and *Atp6ap2*$^{\beta\text{-}ly}$ mice (Fig. 3*E*), despite the concurrent loss of insulin signal (Fig. 3*D*). This data suggests that the loss of insulin$^+$ cells in TAM-treated *Atp6ap2*$^{\beta\text{-}ly}$ mice is not due to increased β cell death at this time point, but to depletion of the insulin stores.

We then measured total insulin and glucagon content in whole pancreas extracts by radioimmunoassay (RIA). After TAM treatment for 8 wk the insulin content of *Atp6ap2*$^{\beta\text{-}ly}$ islets was significantly reduced, while glucagon content was unchanged (Fig. 4*A*).

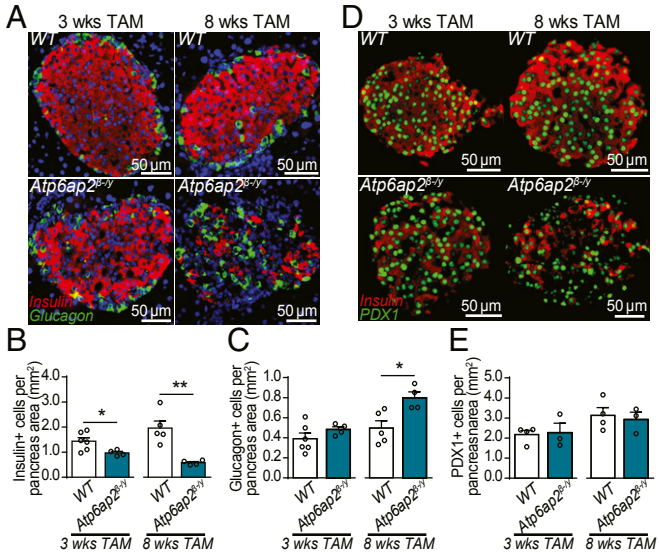

Fig. 3. *Atp6ap2*-deficient β cells have reduced insulin content. (*A*) Islet immunofluorescence for insulin (red) and glucagon (green) of mice after 3 and 8 wk of TAM treatment. Nuclear stain (DAPI) is shown in blue. (*B* and *C*) Quantification of *A*. $n = 4$ to 6. (*D*) Islet immunofluorescence for pancreatic and duodenal homeobox 1 (Pdx1; green) and insulin (red) from mice treated with TAM for 3 and 8 wk. (*E*) Quantification of *D*. $n = 4$ to 6. $^*P < 0.05$, $^{**}P < 0.01$. Scale bars are indicated.

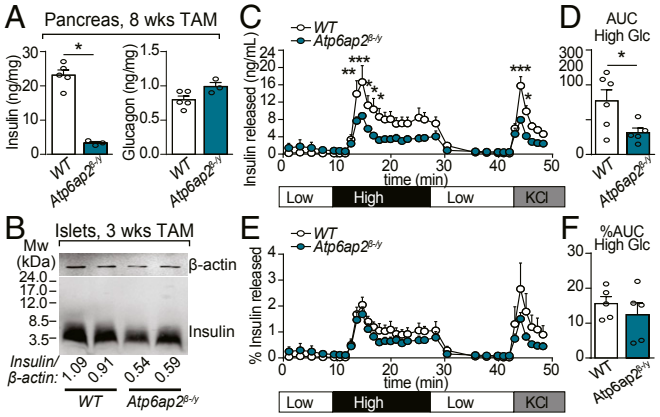

Fig. 4. Insulin processing and secretion is unaltered in *Atp6ap2*$^{\beta\text{-}ly}$ mice. (*A*) Insulin (*Left*) and glucagon (*Right*) content in whole pancreatic extracts from mice treated with TAM for 8 wk. $n = 3$ to 5. (*B*) Insulin processing was analyzed by Western blot in isolated islets from WT and *Atp6ap2*$^{\beta\text{-}ly}$ mice treated with TAM for 3 wk. Molecular weight markers are indicated. The ratio of insulin to loading control (β-actin) is shown normalized to WT. (*C*–*F*) Isolated islets from WT and *Atp6ap2*$^{\beta\text{-}ly}$ mice treated with TAM for 3 wk were perfused with low (3.3 mM), high (16.7 mM), and again low glucose, and then 60 mM KCl. (*C*) Amount of insulin secreted was measured by RIA. (*D*) AUC analysis of high glucose peak from *C*. (*E*) The percentage of insulin released (amount of insulin in *C* divided by total insulin content). (*F*) AUC analysis of high glucose peak from *E*. Three independent experiments with $n = 2$ of each genotype were pooled ($n = 6$ total). $^*P < 0.05$, $^{**}P < 0.01$, $^{***}P < 0.001$.

This finding was confirmed by Western blot of islets isolated from *Atp6ap2*$^{\beta\text{-}ly}$ mice after 3 wk of TAM treatment (Fig. 4*B*). Previous reports suggested that Atp6ap2 is associated with the V-ATPase complex (27, 29, 33). In β cells, this complex is enriched in SGs where it establishes the acidic pH necessary for proinsulin to insulin conversion (34). However, in islets of TAM-treated *Atp6ap2*$^{\beta\text{-}ly}$ mice, proinsulin processing was not affected, as the reduction of mature insulin (~3.5 kDa) did not correlate with increased levels of proinsulin (~7.6 kDa) (Fig. 4*B*).

We next examined the role of Atp6ap2 in insulin SG exocytosis. Islets were isolated from TAM-treated WT and *Atp6ap2*$^{\beta\text{-}ly}$ mice and perfused ex vivo with low glucose (3.3 mM), high glucose (16.7 mM), and low glucose again (3.3 mM), followed by 60 mM KCl, which causes massive membrane depolarization and glucose-independent SG exocytosis. Insulin secretion was measured by RIA. In response to high glucose and KCl, *Atp6ap2*$^{\beta\text{-}ly}$ islets exhibited diminished insulin secretion compared to WT (Fig. 4 *C* and *D*). However, upon normalization for total insulin, the percentage of insulin released by islets from TAM-treated WT or *Atp6ap2*$^{\beta\text{-}ly}$ mice was comparable (Fig. 4 *E* and *F*). These findings indicate that *Atp6ap2* deficiency reduces the insulin content of β cells, without affecting their machinery for SG exocytosis.

Vacuolated Bodies with Intact Acidic pH Consume Cellular Content, Including Insulin SGs. Insulin content in *Atp6ap2*-deficient β cells could be decreased due to reduced insulin production or increased intracellular degradation of insulin. Since insulin mRNA levels in islets of WT and *Atp6ap2*$^{\beta\text{-}ly}$ mice were equivalent (*SI Appendix*, Fig. S1) and considering the extensive vacuolation of *Atp6ap2*-deficient β cells (Fig. 1), we turned our attention to mechanisms of degradation.

Autophagy is a key homeostatic mechanism by which cellular contents are sequestered by a membrane into large vacuoles which then fuse with lysosomes for degradation (5). This process therefore enables the removal of damaged proteins and organelles which could perturb cellular function. In conditions of nutrient deprivation, this degradative pathway is also used to supply amino acids to preserve essential housekeeping cellular activities. A link between Atp6ap2 and autophagy has been suggested

CELL BIOLOGY

because of the elevated expression of autophagy markers in *Atp6ap2*-deficient cells (18, 20, 24), including microtubule-associated protein 1A/1B light chain 3B (*Map1Lc3b* [*LC3B*]), sequestosome 1 (*Sqstm1* or *p62*) and ubiquitin (*Ubq*). Lipidated LC3B binds to double-membraned autophagosomes, while p62 and Ubq bind to protein aggregates destined for encapsulation by autophagosomes. Immunostaining of pancreatic sections for autophagy markers revealed that in islets from 3 and 8 wk TAM-treated *Atp6ap2*$^{\beta\text{-}/y}$ mice areas positive for LC3B, p62, and Ubq were increased relative to islets from WT mice, suggesting an up-regulation of autophagy (Fig. 5 *A–F*). Following their formation, autophagosomes fuse with lysosomes, leading to the formation of autophagolysosomes in which engulfed proteins, organelles and portions of the cytosol are degraded (35). As the accumulation of autophagy markers can indicate an impairment in autophagolysosomal degradation, we next examined whether autophagic flux was impaired. Islets from *Atp6ap2*$^{\beta\text{-}/y}$ mice TAM treated for 3 wk were exposed ex vivo to the V-ATPase inhibitor bafilomycin A1 (BafA1). We determined the abundance of the free cytosolic form of LC3B (LC3B-I) and its lipidated form (LC3B-II), which associates with the autophagosome membrane. Autophagic flux is analyzed by comparing the levels of LC3B-II in cells treated with and without BafA1, as inhibition of the V-ATPase and thus lysosomal acidification leads to accumulation of LC3B-II. Evidence of increased LC3B-II levels prior to BafA1 treatment is indicative of a compromised autophagic flux. LC3B-II levels were slightly increased in islets of TAM-treated *Atp6ap2*$^{\beta\text{-}/y}$ mice (Fig. 5*G*). However, upon BafA1 treatment the accumulation of LC3B-II in islets of WT and *Atp6ap2*$^{\beta\text{-}/y}$ mice was comparable (Fig. 5*G*), suggesting that V-ATPase activity and lysosomal acidification is intact.

We next employed confocal microscopy to more carefully analyze the identity and origin of the large vacuolated structures. We compared the colocalization of autophagosomal (LC3, p62), endosomal (early-endosome antigen 1, EEA1) and lysosomal (lysosomal-associated membrane protein, LAMP1) markers in islets of 8-wk TAM-treated *Atp6ap2*$^{\beta\text{-}/y}$ mice (Fig. 5*H*). LC3B exhibited partial but increased colocalization with the endosomal marker EEA1 and autophagosome marker p62. However, the colocalization of p62 and LC3B to LAMP1 was meager and unchanged compared to WT controls. Together, this analysis suggests that the abnormal vacuolated structures in *Atp6ap2*$^{\beta\text{-}/y}$ islets are likely to originate upstream of the induction of autophagy.

We next turned to Δ*Atp6ap2* INS-1 cells to investigate the nature of the LC3^{+} structures and lysosomal acidification in more detail. Given the limited colocalization between LC3B and LAMP1 in *Atp6ap2*$^{\beta\text{-}/y}$ islets, we first asked whether fusion between autophagosomes and lysosomes to form an autolysosome is impaired. Δ*Atp6ap2* INS-1 cells were transfected to express the fluorescent reporter mCherry-LC3B which localizes to the autophagosome lumen (Fig. 5*I*). This reporter colocalized extensively with an anti-LAMP2 antibody which recognizes a cytoplasmic epitope of the lysosomal marker, therefore accounting for the detection of a ring surrounding the luminal mCherry-LC3B (Fig. 5 *I*, *Inset*). These data imply that *Atp6ap2* deficiency does not preclude the formation of autolysosomes (Fig. 5*I*). We then asked whether inhibiting the induction of autophagy would prevent the formation of these structures. WT and Δ*Atp6ap2* INS-1 cells were treated with the ULK1 protein kinase complex inhibitor MRT 68921 (MRT), which prevents the lipidation of LC3B-II and hence the induction of autophagy. Δ*Atp6ap2* INS-1 cells exhibited increased LC3^{+} structures which were rescued by

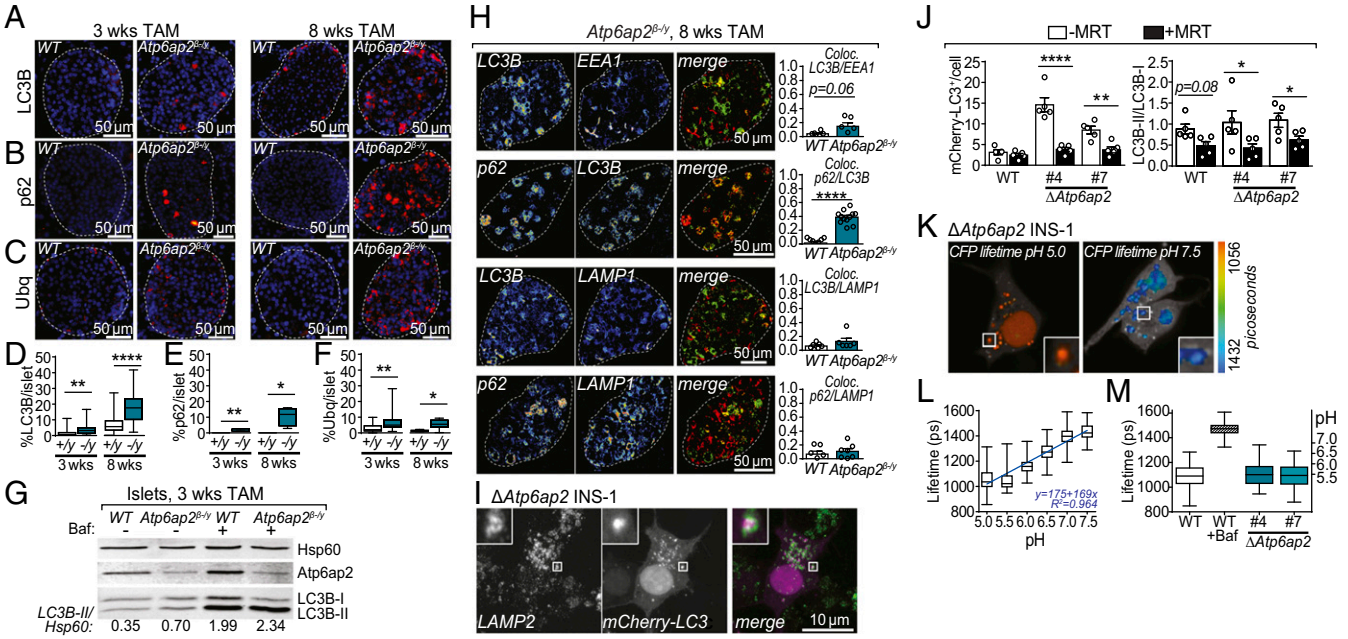

Fig. 5. *Atp6ap2* deletion induces the formation of large vacuoles without impairment of autophagy or lysosomal acidification. (*A–C*) Immunostaining of pancreatic sections from WT and *Atp6ap2*$^{\beta\text{-}/y}$ mice for LC3B (*A*), p62 (*B*), and ubiquitin (*C*) after 3 and 8 wk of TAM treatment. All proteins are depicted in red with a nuclear stain (DAPI) shown in blue. White dashed line indicates total islet area. (*D–F*) Quantification of *A–C* of the % area of positive staining within total islet area. WT are "+/y"; *Atp6ap2*$^{\beta\text{-}/y}$ as "−/y". (*G*) Islets isolated from WT and *Atp6ap2*$^{\beta\text{-}/y}$ mice treated with TAM for 3 wk were cultured ±100 nM Bafilomycin A1 (Baf) for 120 min and then analyzed by Western blotting for expression of LC3B-I, LC3B-II, and Atp6ap2. The ratio of LC3B-II to loading control (Hsp60) is shown. Result is representative of 2 independent experiments. (*H*) Colocalization analysis of LC3B, EEA1, p62, and LAMP1 by immunofluorescence confocal microscopy of WT and *Atp6ap2*$^{\beta\text{-}/y}$ islets treated with TAM for 8 wk. Representative images of *Atp6ap2*$^{\beta\text{-}/y}$ islets are shown with quantitation of colocalization (Pearson's). (*I*) Colocalization analysis of LC3B and LAMP2 by confocal microscopy of Δ*Atp6ap2* INS-1 cells transfected with mCherry-LC3B. (*J*) WT and Δ*Atp6ap2* INS-1 cells were transfected with mCherry-LC3B and incubated ±1 µM MRT 68921 for 12 h. mCherry-LC3B^{+} structures were counted (*Left*) and the ratio of LC3B-II/LC3B-I levels determined by Western blotting (*Right*). (*K* and *L*) LC3B^{+}-vacuolar pH measurements in Δ*Atp6ap2* INS-1 cells by FLIM with calibration to nigericin-buffered solutions from pH 5.0 to 7.5. (*M*) Vacuole pH measurements of WT and 2 independent Δ*Atp6ap2* INS-1 clones were identical while addition of Baf increased vacuolar pH. For all panels, **P* < 0.05; ***P* < 0.01; *****P* < 0.0001.

treatment with MRT and associated with a decreased LC3B-II/LC3B-I ratio (Fig. 5*J*). We finally sought to measure the pH of $LC3B^+$ structures by fluorescence lifetime imaging microscopy (FLIM) utilizing the pH sensitivity of CFP (36, 37). To this aim we generated a CFP-LC3B fusion protein and measured the CFP lifetime in Δ*Atp6ap2* INS-1 cells cultured in nigericin-buffered solutions ranging from pH 5.0 to 7.5 (Fig. 5 *K* and *L*). During autophagosome formation, CFP-LC3B is lipidated with a fraction remaining attached to the luminal side of the autophagosome membrane. As the intracellular fluorescence lifetime of CFP undergoes large linear changes in this pH range, CFP-LC3B can be used to accurately measure the pH in the $LC3B^+$ structures. As these $LC3B^+$ structures also colocalize with LAMP2 (Fig. 5*I*), this method thus allows the measurement of autophagosome/autophagolysosome pH. The sensitivity of this reporter was confirmed by evidence that exposure of WT INS-1 cells to BafA1 increased the vacuolar pH from ∼5.5 to 7.0 (Fig. 5*M*). In both Δ*Atp6ap2* INS-1 clones, $LC3B^+$ structures had an acidic pH, with no significant difference to those in WT INS-1 cells (Fig. 5*M*). These data suggest that *Atp6ap2* deletion does not perturb V-ATPase activity. We also measured more broadly the effect of *ATP6AP2* silencing on lysosomal acidification in HeLa cells, by assessing EGF-induced EGFR recycling and cathepsin maturation (*SI Appendix*, Fig. S7). In all assays, control siRNA did not affect lysosomal acidification while the addition of BafA1 completely blocked V-ATPase activity as evidenced by a reduction in LysoTracker fluorescence intensity, inhibited EGFR degradation, and reduced Cathepsin L activity (*SI Appendix*, Fig. S7). By contrast, *ATP6AP2*-silenced cells did not exhibit any difference to control siRNA and further corroborating that *ATP6AP2* deficiency does not affect lysosomal acidification (*SI Appendix*, Fig. S7).

Discussion

Disturbances in insulin SG trafficking and turnover can have profound consequences on cellular homeostasis of the β cell. Despite intact autophagy and acidification mechanisms in $Atp6ap2^{\beta\text{-}/y}$ islets, our results suggest that the major consequence of *Atp6ap2* deficiency is the exacerbated generation and accumulation of multigranular bodies that consume the cytoplasm of β cells, ensnaring insulin SGs and thus causing insulin-deficient diabetes (*SI Appendix*, Fig. S8).

Atp6ap2 was discovered more than a decade ago and initially named the (pro)renin receptor, as it was thought to be functionally associated with the renin-angiotensin system (RAS) (15). It has subsequently been realized that Atp6ap2 is important for many other cellular functions independent of the RAS, and it is now becoming clear that the primary function of Atp6ap2 is not directly associated with this system; rather, it has a ubiquitous and essential role in maintaining cellular homeostasis (16, 38). In the years since its discovery, much effort has been directed toward the characterization of signaling pathways that are "controlled" by Atp6ap2. These include Wnt (25–27) and promyelocytic leukemia zinc finger (PLZF) (39) signaling, despite a lack of similarity between the respective in vivo models (21), and that employed concentrations of its "ligands" renin and (pro)renin were several orders of magnitude above circulating levels (16). Abnormal vacuolar phenotypes are evident upon conditional Atp6ap2 knockout from cardiomyocytes (19), podocytes (18, 20), and hepatocytes (24). Considering this literature with the results presented here, an explanation for why loss of Atp6ap2 affects so many pathways and cell types may be because of the cell "constipation" by vacuolated structures, with loss of homeostasis and thus inability to retain normal signaling function. This interpretation is supported by our finding that while $Atp6ap2^{\beta\text{-}/y}$ islets secrete reduced amounts of insulin in response to high glucose, this difference is lost when normalized for the total insulin content, indicating that what insulin is left can be secreted by the β cell. This essentiality of Atp6ap2 for cellular homeostasis should be carefully considered when evaluating its role in pathological processes. The fact that its deletion attenuates fibrosis in diabetic heart disease (40) and abolishes brain-RAS responses (41), may simply be due to the loss of homeostasis experienced by *Atp6ap2*-deficient cells, rendering them similarly unable to mount pathological responses. This may also explain why elevated expression of Atp6ap2 is associated with cellular insult (40, 42, 43) as subsequent increases in homeostatic mechanisms are thereafter induced to prevent disease.

Our study identifies Atp6ap2 as an important player in insulin homeostasis. While Atp6ap2 has been found to colocalize with the V-ATPase (28, 29), findings by us and others (28) suggest that this association is not required for the V-ATPase-driven acidification of SGs and lysosomes. This conclusion is supported by comparison of the phenotypic traits observed here in *Atp6ap2*-deficient β cells with those of *V-ATPase*-deficient β cells, which reported impaired processing of proinsulin to insulin (14) and decreased plasma insulin, attenuated glucose- and potassium-stimulated insulin secretion with normal islet and β cell morphology (13, 14). In stark contrast, we show that deletion of *Atp6ap2* in β cells results in slightly increased fasted plasma insulin, no abnormalities in proinsulin processing, decreased insulin content with no impairment in SG release, and a severely disturbed vacuolated β cell morphology. Moreover, using the newly generated pH reporter CFP-LC3B for FLIM we found that *Atp6ap2*-deficient β cell lysosomes were acidic, but still susceptible to alkalinization upon BafA1 treatment, which inhibits V-ATPase function. Recent high-resolution atomic models of the V_0 subunit of the yeast V-ATPase complex by electron cryomicroscopy has given new molecular insight into its proton translocation mechanism; notably, ATP6AP2 was absent from both structures as there is no known yeast homolog (44, 45). Elucidation of the fully assembled V_0V_1-ATPase from higher order eukaryotes will be important to determine if Atp6ap2 directly associates with this complex and if so, to reveal the functional implications of its association.

While markers of autophagy are increased in $Atp6ap2^{\beta\text{-}/y}$ cells, we find mechanisms underpinning autophagy induction and flux to be functional here, although grossly overloaded. Atp6ap2 has been proposed to modulate the activity of autophagy-regulator mammalian target of rapamycin (mTOR) (31). However, mTOR complex 1 (MTORC1)-deficient β cells of $\beta ra^{-/-}$ mice display a very different phenotype from the *Atp6ap2*-deficient β cells described here. In particular they accumulate lysosomes filled with SGs, with apoptosis and loss of β cell mass (46). Likewise, $Atg7^{\Delta\beta}$ mice which are unable to generate LC3B-II and therefore have a deficiency in autophagosome formation, show decreased serum insulin and compromised GSIS (6). By contrast, the phenotype of $Atp6ap2^{\beta\text{-}/y}$ mice is more reminiscent of that of $Rab3A^{-/-}$ mice, which lack a GTP-binding protein important for vesicular trafficking (47). $Rab3A^{-/-}$ β cells exhibit increased insulin degradation, with the accumulation of vacuolated structures and up-regulation of both autophagy and crinophagy (47). Similarly, podocyte-specific deletion of vacuolar protein sorting 34 (*Vps34*) resulted in the accumulation of large, single-membraned vacuoles due to impaired vesicle fusion and maturation (48). Our analyses of the identity of $Atp6ap2^{\beta\text{-}/y}$ vacuolated structures indicated that they originate upstream of the induction of autophagy, as evidenced by partial colocalization with endosomal and early autophagy markers and that the formation of $LC3^+$ vacuoles was prevented in *Atp6ap2*-deficient INS-1 cells treated with an ULK1 inhibitor. That these structures contain luminal LC3 and are prevented by ULK1 inhibition also rules out their identity as LC3-associated phagocytosis (LAP) phagosomes (5). Taken together, and because of the disparities between V-ATPase- and autophagy-deficient mice, we hypothesize that Atp6ap2 is important for restraining SG fusion or trafficking upstream of the induction of autophagy. Accordingly, its deletion in β cells, which wholly focus on insulin SG exocytosis and recycling, leads to a very severe phenotype in which large vacuoles accumulate that feed into the autophagy pathway and results in the degradation of insulin. In line with this view, Kissing et al.

observed increased fusion rates between phagosomes with lysosomes in *Atp6ap2*-deficient macrophages which were not associated with impaired lysosomal acidification (49). Further, *Atp6ap2* was recently found to coimmunoprecipitate with sortilin-1, a protein required for transport between the endoplasmic reticulum, the Golgi complex, and endolysosomal compartments (50). While distinct from acidification, it may still be that Atp6ap2's role in vesicular trafficking is driven by an association with the V-ATPase.

Methods

Detailed descriptions are provided in *SI Appendix, SI Materials and Methods*.

Animal experiments were approved by the Landesamt für Gesundheit und Soziales, Berlin, Germany. *Atp6ap2*$^{\beta\text{-}ly}$ mice (male) were generated by crossing female *Atp6ap2* floxed mice (*Atp6ap2*$^{flox/+}$) with male *RIP-CreER* mice. Tamoxifen pellets (25 mg/pellet, Innovative Research of America) were inserted s.c. IPGTTs were performed as previously described (51). Whole pancreases were dissected, fixed, embedded, and stained for TEM and immunofluorescence microscopy. Islets were isolated from the pancreases of WT and *Atp6ap2*$^{\beta\text{-}ly}$ mice treated with TAM for 3 wk by collagenase digestion and subsequent centrifugation through a Histopaque gradient. Isolated islets were then cultured overnight in media (RPMI containing 10% FCS and 1% penicillin/streptomycin) at 37 °C with 5% CO_2. Islets were then assayed for insulin secretion, Western blotting, or real-time PCR. *Atp6ap2* INS-1 knockout clones were generated as described (52) and assayed by microscopy, Western blotting, and for vacuole pH measurements.

ACKNOWLEDGMENTS. We thank Jana Czychi, Ilona Kamer, Francesca Spagnoli, and Thomas Rathjen (all MDC-Berlin), Prof. Gil Leibowitz (The Hebrew University of Jerusalem), Prof. Paul Gleeson (The University of Melbourne), and Anthony Rousselle for generously providing the *Atp6ap2*$^{flox/+}$;*R26YFP*$^{flox/flox}$ mice (MDC-Berlin). K.J.B. was funded for this study by an Australian National Health Medical Research Council (NHMRC) fellowship (APP1037633). A.L.B. and D.M.W. were supported by the German Research Foundation (BI1292/4-2, BI1292/9-1, BI1292/10-1, BI1292/12-1, and IRTG2251). D.N.M. was supported by the German Research Foundation (DFG; 394046635 - SFB1365) and the German Center for Cardiovascular Research. M.N. was supported by a Dresden International Graduate School for Biomedicine and Bioengineering (DIGS-BB) PhD fellowship. M.S. was supported by the German Federal Ministry of Education and Research (BMBF) to the German Center for Diabetes Research and by the German–Israeli Foundation (I-1429-201.2/2017).

1. G. C. Weir, S. Bonner-Weir, Five stages of evolving beta-cell dysfunction during progression to diabetes. *Diabetes* **53** (suppl. 3), S16–S21 (2004).
2. E. Fava *et al*., Novel standards in the measurement of rat insulin granules combining electron microscopy, high-content image analysis and in silico modelling. *Diabetologia* **55**, 1013–1023 (2012).
3. A. Müller, H. Mziaut, M. Neukam, K.-P. Knoch, M. Solimena, A 4D view on insulin secretory granule turnover in the β-cell. *Diabetes Obes. Metab.* **19** (suppl. 1), 107–114 (2017).
4. L. Orci *et al*., Insulin, not C-peptide (proinsulin), is present in crinophagic bodies of the pancreatic B-cell. *J. Cell Biol.* **98**, 222–228 (1984).
5. K. Cadwell, J. Debnath, Beyond self-eating: The control of nonautophagic functions and signaling pathways by autophagy-related proteins. *J. Cell Biol.* **217**, 813–822 (2018).
6. H. S. Jung *et al*., Loss of autophagy diminishes pancreatic beta cell mass and function with resultant hyperglycemia. *Cell Metab.* **8**, 318–324 (2008).
7. C. Ebato *et al*., Autophagy is important in islet homeostasis and compensatory increase of beta cell mass in response to high-fat diet. *Cell Metab.* **8**, 325–332 (2008).
8. M. Masini *et al*., Autophagy in human type 2 diabetes pancreatic beta cells. *Diabetologia* **52**, 1083–1086 (2009).
9. S. Wang, Q.-q. Sun, B. Xiang, X.-J. Li, Pancreatic islet cell autophagy during aging in rats. *Clin. Invest. Med.* **36**, E72–E80 (2013).
10. E. Bell *et al*., Rapamycin has a deleterious effect on MIN-6 cells and rat and human islets. *Diabetes* **52**, 2731–2739 (2003).
11. M. Tanemura *et al*., Rapamycin causes upregulation of autophagy and impairs islets function both in vitro and in vivo. *Am. J. Transplant.* **12**, 102–114 (2012).
12. R. A. Oot, S. Couoh-Cardel, S. Sharma, N. J. Stam, S. Wilkens, Breaking up and making up. The secret life of the vacuolar H+ -ATPase. *Protein Sci.* **26**, 896–909 (2017).
13. G.-H. Sun-Wada *et al*., The a3 isoform of V-ATPase regulates insulin secretion from pancreatic beta-cells. *J. Cell Sci.* **119**, 4531–4540 (2006).
14. E. Louagie *et al*., Role of furin in granular acidification in the endocrine pancreas. Identification of the V-ATPase subunit Ac45 as a candidate substrate. *Proc. Natl. Acad. Sci. U.S.A.* **105**, 12319–12324 (2008).
15. G. Nguyen *et al*., Pivotal role of the renin/prorenin receptor in angiotensin II production and cellular responses to renin. *J. Clin. Invest.* **109**, 1417–1427 (2002).
16. D. J. Campbell, Critical review of prorenin and (pro)renin receptor research. *Hypertension* **51**, 1259–1264 (2008).
17. C. Burckle, M. Bader, Prorenin and its ancient receptor. *Hypertension* **48**, 549–551 (2006).
18. Y. Oshima *et al*., Prorenin receptor is essential for normal podocyte structure and function. *J. Am. Soc. Nephrol.* **22**, 2203–2212 (2011).
19. K. Kinouchi *et al*., The (pro)renin receptor/ATP6AP2 is essential for vacuolar H+-ATPase assembly in murine cardiomyocytes. *Circ. Res.* **107**, 30–34 (2010).
20. F. Riediger *et al*., Prorenin receptor is essential for podocyte autophagy and survival. *J. Am. Soc. Nephrol.* **22**, 2193–2202 (2011).
21. S. Geisberger *et al*., New role for the (pro)renin receptor in T-cell development. *Blood* **126**, 504–507 (2015).
22. R. Song, G. Preston, A. Ichihara, I. V. Yosypiv, Deletion of the prorenin receptor from the ureteric bud causes renal hypodysplasia. *PLoS One* **8**, e63835 (2013).
23. F. Trepiccione *et al*., Renal Atp6ap2/(Pro)renin receptor is required for normal vacuolar H+-ATPase function but not for the renin-angiotensin system. *J. Am. Soc. Nephrol.* **27**, 3320–3330 (2016).
24. S. Kissing *et al*., Disruption of the vacuolar-type H^+-ATPase complex in liver causes MTORC1-independent accumulation of autophagic vacuoles and lysosomes. *Autophagy* **13**, 670–685 (2017).
25. T. Hermle, D. Saltukoglu, J. Grünewald, G. Walz, M. Simons, Regulation of Frizzled-dependent planar polarity signaling by a V-ATPase subunit. *Curr. Biol.* **20**, 1269–1276 (2010).
26. T. Hermle, M. C. Guida, S. Beck, S. Helmstädter, M. Simons, Drosophila ATP6AP2/VhaPRR functions both as a novel planar cell polarity core protein and a regulator of endosomal trafficking. *EMBO J.* **32**, 245–259 (2013).
27. C.-M. Cruciat *et al*., Requirement of prorenin receptor and vacuolar H+-ATPase-mediated acidification for Wnt signaling. *Science* **327**, 459–463 (2010).
28. A. Daryadel *et al*., Colocalization of the (Pro)renin Receptor/Atp6ap2 with H+-ATPases in mouse kidney but prorenin does not acutely regulate intercalated cell H+-ATPase activity. *PLoS One* **11**, e0147831 (2016).
29. A. Advani *et al*., The (Pro)renin receptor. Site-specific and functional linkage to the vacuolar H+-ATPase in the kidney. *Hypertension* **54**, 261–269 (2009).
30. M. C. Guida *et al*., ATP6AP2 functions as a V-ATPase assembly factor in the endoplasmic reticulum. *Mol. Biol. Cell* **29**, 2156–2164 (2018).
31. K. J. Binger, D. N. Muller, Autophagy and the (Pro)renin receptor. *Front. Endocrinol.(Lausanne)* **4**, 155 (2013).
32. D. Schvartz *et al*., Improved characterization of the insulin secretory granule proteomes. *J. Proteomics* **75**, 4620–4631 (2012).
33. J. Ludwig *et al*., Identification and characterization of a novel 9.2-kDa membrane sector-associated protein of vacuolar proton-ATPase from chromaffin granules. *J. Biol. Chem.* **273**, 10939–10947 (1998).
34. L. Orci *et al*., Conversion of proinsulin to insulin occurs coordinately with acidification of maturing secretory vesicles. *J. Cell Biol.* **103**, 2273–2281 (1986).
35. E.-L. Eskelinen, P. Saftig, Autophagy: A lysosomal degradation pathway with a central role in health and disease. *Biochim. Biophys. Acta* **1793**, 664–673 (2009).
36. S. Poëa-Guyon *et al*., The V-ATPase membrane domain is a sensor of granular pH that controls the exocytotic machinery. *J. Cell Biol.* **203**, 283–298 (2013).
37. M. Neukam, A. Soenmez, M. Solimena, FLIM-based pH measurements reveal incretin-induced rejuvenation of aged insulin secretory granules. bioRxiv:10.1101/174391 (9 November 2017).
38. W. W. Batenburg, A. H. J. Danser, (Pro)renin and its receptors. Pathophysiological implications. *Clin. Sci.* **123**, 121–133 (2012).
39. J. H. Schefe *et al*., A novel signal transduction cascade involving direct physical interaction of the renin/prorenin receptor with the transcription factor promyelocytic zinc finger protein. *Circ. Res.* **99**, 1355–1366 (2006).
40. S. Yu *et al*., (Pro)renin receptor RNAi silencing attenuates diabetic cardiomyopathy pathological process in rats. *Hum. Gene Ther.* **30**, 727–739 (2019).
41. W. Li *et al*., Neuron-specific (pro)renin receptor knockout prevents the development of salt-sensitive hypertension. *Hypertension* **63**, 316–323 (2014).
42. J. L. Wilkinson-Berka *et al*., RILLKKMPSV influences the vasculature, neurons and glia, and (pro)renin receptor expression in the retina. *Hypertension* **55**, 1454–1460 (2010).
43. A. A. Gonzalez, L. S. Lara, C. Luffman, D. M. Seth, M. C. Prieto, Soluble form of the (pro)renin receptor is augmented in the collecting duct and urine of chronic angiotensin II-dependent hypertensive rats. *Hypertension* **57**, 859–864 (2011).
44. S.-H. Roh *et al*., The 3.5-Å CryoEM structure of nanodisc-reconstituted yeast vacuolar ATPase V_o proton channel. *Mol. Cell* **69**, 993–1004.e3 (2018).
45. M. T. Mazhab-Jafari *et al*., Atomic model for the membrane-embedded V_O motor of a eukaryotic V-ATPase. *Nature* **539**, 118–122 (2016).
46. M. Blandino-Rosano *et al*., Loss of mTORC1 signalling impairs β-cell homeostasis and insulin processing. *Nat. Commun.* **8**, 16014 (2017).
47. B. J. Marsh *et al*., Regulated autophagy controls hormone content in secretory-deficient pancreatic endocrine beta-cells. *Mol. Endocrinol.* **21**, 2255–2269 (2007).
48. W. Bechtel *et al*., Vps34 deficiency reveals the importance of endocytosis for podocyte homeostasis. *J. Am. Soc. Nephrol.* **24**, 727–743 (2013).
49. S. Kissing *et al*., Vacuolar ATPase in phagosome-lysosome fusion. *J. Biol. Chem.* **290**, 14166–14180 (2015).
50. X. Lu *et al*., Identification of the (Pro)renin receptor as a novel regulator of low-density lipoprotein metabolism. *Circ. Res.* **118**, 222–229 (2016).
51. A. L. Birkenfeld *et al*., Deletion of the mammalian INDY homolog mimics aspects of dietary restriction and protects against adiposity and insulin resistance in mice. *Cell Metab.* **14**, 184–195 (2011).
52. F. A. Ran *et al*., Genome engineering using the CRISPR-Cas9 system. *Nat. Protoc.* **8**, 2281–2308 (2013).